Meson production in two-photon interactions at energies available at the CERN Large Hadron Collider

V. P. Gonçalves, D. T. da Silva, and W. K. Sauter
Instituto de Física e Matemática, Universidade Federal de Pelotas Caixa Postal 354, CEP 96010-900, Pelotas, RS, Brazil
(Received 28 August 2012; revised manuscript received 19 December 2012; published 4 February 2013)

The meson production cross sections are estimated considering photon-photon interactions in hadron-hadron collisions at CERN Large Hadron Collider (LHC) energies. We consider a large number of mesons with photon-photon partial decay width well constrained by the experiment and some mesons which are currently considered as hadronic molecule and glueball candidates. Our results demonstrate that the experimental analysis of these states is feasible at the CERN LHC.

DOI: 10.1103/PhysRevC.87.028201 PACS number(s): 13.85.Ni, 12.40.Nn, 13.85.Qk, 13.87.Ce

The Large Hadron Collider (LHC) at CERN started high energy collisions two years ago. During this period a large amount of data have been collected considering pp collisions at $\sqrt{s} = 0.9$, 2.36, and 7 TeV as well as PbPb collisions at $\sqrt{s} = 2.76$ TeV. Currently, there is a great expectation that LHC will discover new physics beyond the standard model, such as supersymmetry or extra dimensions. However, we should remember that the LHC opens a new kinematical regime at high energy, where several questions related to the description of the quantum chromodynamics (QCD) remain without satisfactory answers. Some open questions are the search for non-$q\bar{q}$ resonances, the determination of the spectrum of $q\bar{q}$ states and the identification of states with anomalous $\gamma\gamma$ couplings. A possible way to study these problems is the study of meson production in two-photon interactions [1,2]. In general, this process is studied in leptonic colliders. An alternative is to use ultrarelativistic protons and nuclei, which give rise to strong electromagnetic fields and estimate the production of a given final state considering the photon-photon and photon-hadron interactions. In particular, it is possible to study photon-photon interactions in proton-proton and nucleus-nucleus collisions at LHC (for a review see Ref. [3]). Recently, Bertulani [4] revisited this subject and proposed the study of the meson production in ultraperipheral heavy ion collisions at LHC in order to constrain the two-photon decay widths. In this Brief Report we extend this previous study for the meson production in two-photon interactions in proton-proton collisions. Initially we calculate the cross sections for mesons with photon-photon partial decay width well constrained by the experiment, which allows to constrain the theoretical methods and calibrates the experimental techniques. After we predict the cross sections for mesons which are currently considered as glueball and hadronic molecule candidates. Our results shows that LHC can be used to investigate these states.

Let us consider the hadron-hadron interaction at large impact parameter ($b > R_{h_1} + R_{h_2}$) and at ultrarelativistic energies (for recent reviews see, e.g., Ref. [5]). In this regime we expect the electromagnetic interaction to be dominant. In heavy ion colliders, the heavy nuclei give rise to strong electromagnetic fields due to the coherent action of all protons in the nucleus, which can interact with each other. In a similar way, it also occurs when considering ultra relativistic protons in $pp(\bar{p})$ colliders. The photon stemming from the electromagnetic field of one of the two colliding hadrons can interact with one photon of the other hadron (two-photon process) or can interact directly with the other hadron (photon-hadron process). The total cross section for a given process can be factorized in terms of the equivalent flux of photons of the hadron projectile and the photon-photon or photon-target production cross section. In the case of the production of a neutral state X in two-photon interactions the total cross section is given by (see, e.g., Ref. [6])

$$\sigma(h_1 h_2 \to h_1 \otimes X \otimes h_2) = \int dx_1 \int dx_2 f^{\gamma}_{h_1}(x_1) f^{\gamma}_{h_2}(x_2) \sigma^{X}_{\gamma\gamma}(x_1 x_2 s), \quad (1)$$

where $\otimes$ characterizes the presence of a rapidity gap in the final state, s is the squared center of mass energy, $f^{\gamma}_{h_i}$ is the distribution function which is associated to the flux of photons generated by the hadron h_i ($i = 1, 2$), $x_i = \omega_i / E_i$, with ω_i and E_i the photon and hadron energies, respectively. Moreover, $\sigma^{X}_{\gamma\gamma}$ is the photon-photon cross section given by

$$\sigma^{X}_{\gamma\gamma}(x_1 x_2 s) = 8\pi^2 (2J+1) \frac{\Gamma_{X\to\gamma\gamma}}{m_X} \delta\left(x_1 x_2 s - m_X^2\right), \quad (2)$$

where J, m_X, and $\Gamma_{X\to\gamma\gamma}$ are the spin, mass and the photon-photon partial decay width of the final state X, respectively, and the δ function enforces energy conservation.

The main input in our calculations are the equivalent photon flux for a ultrarelativistic proton, $f^{\gamma}(x)$, and the two photon partial decay widths, $\Gamma_{X\to\gamma\gamma}$. Currently there are different models for the equivalent photon flux available in the literature (see, e.g., Ref. [7]). The general expression for the equivalent photon flux of an extended object is given by [6]

$$f^{\gamma}(x) = \frac{\alpha Z^2}{\pi} \frac{1 - x + 0.5x^2}{x} \int_{Q^2_{\rm min}}^{\infty} dQ^2 \frac{Q^2 - Q^2_{\rm min}}{Q^4} |F(Q^2)|^2, \quad (3)$$

where Q^2 is the momentum transfer from the projectile and $F(Q^2)$ its form factor. Moreover, $Q^2_{\rm min} \approx (x M_A)^2/(1-x)$ with M_A the mass of the projectile. The presence of the form factor cuts off the photon flux above $1 \simeq 2$ GeV^2. As its dependence on the photon virtuality is $\approx 1/Q^2$, the average

virtuality is very small, which allow us to treat the processes as due to quasireal photon photon collisions.

Considering only the electric dipole form factor for the proton, $F_E(Q^2) = 1/(1 + Q^2/0.71\,\mathrm{GeV}^2)^2$, the following expression for the equivalent photon flux can be obtained:

$$f_h^\gamma(x) = \frac{\alpha}{\pi}\left(\frac{1 - x + 0.5x^2}{x}\right) \times \left[\frac{A+3}{A-1}\ln(A) - \frac{17}{6} - \frac{4}{3A} + \frac{1}{6A^2}\right], \quad (4)$$

where $A = 1 + (0.71\mathrm{GeV}^2)/Q^2_{\mathrm{min}}$. We denote this model by *Electric* in what follows. If the term containing Q^2_{min} in Eq. (3) is disregarded, the equivalent photon spectrum of high energy protons is given as

$$f_h^\gamma(x) = \frac{\alpha}{\pi}\left(\frac{1 - x + 0.5x^2}{x}\right) \times \left[\ln(A) - \frac{11}{6} + \frac{3}{A} - \frac{3}{2A^2} + \frac{1}{3A^3}\right]. \quad (5)$$

This expression was derived originally by Dress and Zeppenfeld in Ref. [8] and will be denoted DZ hereafter. In Ref. [9], the author studied the effect of including the magnetic dipole moment and the corresponding magnetic form factor of the proton, obtaining a spectrum (denoted *Electric + Magnetic* hereafter) which is smaller than the DZ one at small x. Another model considered in literature is the use of a minimum impact parameter, $b_{\mathrm{min}} = 0.7$ fm, in the photon energy spectrum produced by a point particle, which is given by

$$f^\gamma(x) = \frac{\alpha Z^2}{\pi x}\left[2\xi K_0(\xi)K_1(\xi) - \xi^2\left(K_1^2(\xi) - K_0^2(\xi)\right)\right], \quad (6)$$

where K_0 and K_1 are modified Bessel functions and $\xi \equiv x M_A b_{\mathrm{min}}$. In Fig. 1 we present a comparison between these different models for the photon flux. A basic characteristic of the distinct models for the photon spectrum is that they diminish with energy approximately like $1/x$. Consequently, the photon spectrum is strongly peaked at low x, so that the photon-photon center of mass energy, $\approx 2\sqrt{\omega_1\omega_2}$, is much smaller than the center of mass energy of the proton-proton system. Therefore, the main contribution for the total cross section, Eq. (1) comes from the small x behavior of the photon spectrum. In this region, the DZ model predicts a larger photon flux. In contrast, the *Electric* one, predicts the lower photon flux. The other two models, the *Electric + Magnetic* and $b_{\mathrm{min}} = 0.7$ fm models, predict intermediate values for the photon flux. At low x ($\leqslant 0.05$) the difference between the models is ever smaller than 20 %. However, the difference increases at larger values of x. At $x = 0.1$ the difference among the DZ and *Electric* models is $\approx$25%, increasing for $\approx$100% at $x = 0.4$. In this letter we will use the *Electric* and DZ photon fluxes in our calculations, which allow us to estimate the theoretical uncertainty in our predictions.

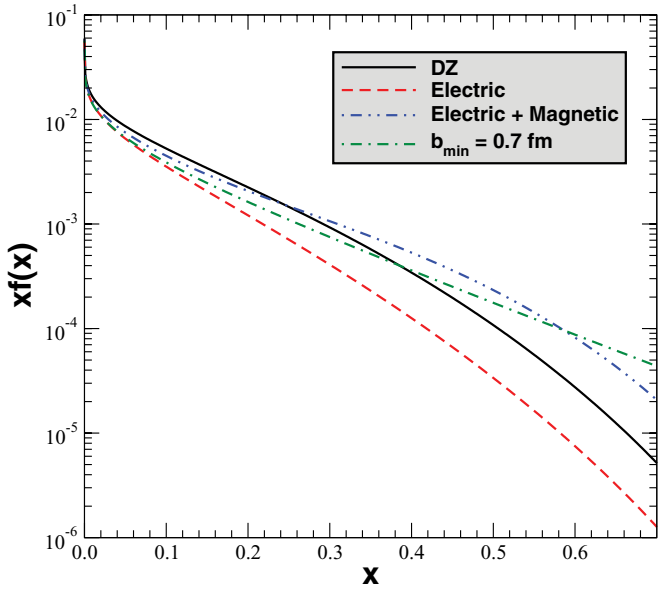

FIG. 1. (Color online) Comparison between different models for the equivalent photon flux as a function of the fractional photon energy x.

In what follows we present our predictions for the total cross section considering proton-proton collisions at LHC and center of mass energies of 7 TeV and 14 TeV. We consider $\Gamma_{\gamma\gamma}$ either taken from experiment or from theory. Initially, we present in Table I our predictions for the mesons which have partial decay ratio reasonably well constrained by the experiment, which allows to use the values present in the Particle Data Group [10]. As emphasized before, the study of mesons which have its decay ratio well known is fundamental to constrain the theoretical methods and calibrate the experimental techniques, for in a second moment investigate the production of exotic particles. As expected from Eqs. (1) and (2), the cross sections decrease at larger values of the meson mass m_X and increase at larger values of $\Gamma_{\gamma\gamma}$. Moreover, the cross sections increase by $\approx$ 30% when the center of mass energy increases from 7 to 14 TeV. The difference between the *Electric* and DZ depends of the final state and it is of the order of $\approx$20%. Assuming

TABLE I. Cross sections for meson production at LHC energies considering the partial decay rates given by the Particle Data Group [10].

State	$\Gamma^{\mathrm{exp}}_{\gamma\gamma}$(keV)	$\sigma_{Electric}$ (pb)		σ_{DZ} (pb)	
	$X \to \gamma\gamma$	7 TeV	14 TeV	7 TeV	14 TeV
π^0	$(8.3 \pm 0.49) \times 10^{-3}$	2426.0	3008.0	2812.0	3453.9
η	0.510 ± 0.026	1368.9	1760.0	1624.8	2062.9
η'	4.29 ± 0.14	1730.6	2265.9	2078.0	2682.0
$f_0(980)$	$0.29^{+0.07}_{-0.06}$	108.0	141.8	130.0	167.9
$a_0(980)$	0.30 ± 0.10	111.9	146.7	134.0	173.7
$f_2(1270)$	3.03 ± 0.35	2300.8	3043.9	2781.0	3623.7
$a_2(1320)$	1.0 ± 0.06	677.8	897.8	820.0	1069.6
$f_2'(1525)$	0.081 ± 0.009	33.0	44.0	40.0	53.0
$f_2(1565)$	0.70 ± 0.14	264.9	353.0	321.9	422.0
$a_2(1700)$	0.30 ± 0.05	79.6	106.6	97.0	127.7
$f_2(1750)$	0.13 ± 0.04	33.0	44.0	40.0	52.9
$\eta_c(1S)$	$6.7^{+0.9}_{-0.8}$	58.0	80.0	72.0	97.0
$\chi_{c0}(1P)$	2.28 ± 0.3	11.0	15.9	14.0	19.0
$\chi_{c2}(1P)$	0.504 ± 0.06	11.0	15.0	13.7	18.6
$\eta_c(2S)$	1.30 ± 0.6	5.0	7.0	6.0	8.9

TABLE II. Cross sections and event rates for meson production considering theoretical decay rates presented in Ref. [4].

State	$\Gamma_{\gamma\gamma}^{\text{theor}}$(keV)	$\sigma_{Electric}$ (pb)		σ_{DZ} (pb)	
	$X \to \gamma\gamma$	7 TeV	14 TeV	7 TeV	14 TeV
$\pi(1300)$	0.43	61.10	80.89	73.90	96.34
$f_4(2050)$	0.36	101.52	136.80	124.18	164.47
$\eta_b(1S)$	0.17	0.024	0.035	0.031	0.044
$\chi_{b0}(1P)$	13.0×10^{-3}	0.0015	0.0022	0.0019	0.0028
$\chi_{b2}(1P)$	3.7×10^{-3}	0.0021	0.0031	0.0027	0.0039

the design luminosity $\mathcal{L} = 10^7$ mb^{-1} s^{-1} the corresponding event rates will be larger than 10^5 events/year at $\sqrt{s} = 7$ TeV, making the experimental analysis of these final states feasible at LHC.

In Tables II–IV we present our predictions for some mesons that does not have two photon partial decay rates well constrained by the experiment. Our goal now is to verify if the study of the meson production in two-photon interactions at LHC can be used to constrain the partial decay rates and, consequently, the theoretical models considered in our calculations. In Table II we consider the theoretical values for $\Gamma_{\gamma\gamma}$ as given in [4]. The small values of $\Gamma_{\gamma\gamma}$ for the χ_{b0} and χ_{b2} states implies that the experimental analysis of these states is a hard task.

Recently, several new observed states have been interpreted as being hadronic molecules, i.e., bound states of two or more mesons (for a review see, e.g., Ref. [11]). In these models two photon radiative decays are considered diagnostic tools which are sensitive to the inner structure of the short-lived molecules. Here we consider the model proposed in Refs. [13–15], where the decay rates are obtained considering an effective Lagrangian which includes both the coupling of the molecular bound state to their hadronic constituents and the coupling of the constituents to other hadrons and photons. For instance, in this model the $X(3940)$ meson is considered as a superposition of the molecular $D^{*+}D^{*-}$ and $D^{*0}D^{*0}$ states, while the $X(4140)$ meson is a bound state of D_s^{*+} and D_s^{*-} mesons. In Table III we present our predictions for some hadronic molecule candidates considering the two-photon decay rates given in Refs. [13–15]. We assume that the masses of the mesons $f_0(1370)$, $f_0(1710)$, $X(3940)$, and $X(4140)$ are given by 1523, 1721, 3943, and 4143 MeV, respectively. For

TABLE III. Cross sections for hadronic molecule candidates at LHC energies considering the theoretical decay rates predicted in Refs. [13–15].

State	Mass	$\Gamma_{\gamma\gamma}^{\text{theor}}$(keV)	$\sigma_{Electric}$ (pb)		σ_{DZ} (pb)	
	(MeV)	$H \to \gamma\gamma$	7 TeV	14 TeV	7 TeV	14 TeV
$f_0(1370)$	1523	1.3	108.7	144.1	131.3	172.2
$f_0(1710)$	1721	0.05	2.7	3.6	3.3	4.4
$X(3940)$, 0^{++}	3943	0.33 ± 0.01	1.01	1.4	1.3	1.7
$X(3940)$, 2^{++}	3943	0.27 ± 0.01	4.1	5.7	5.1	7.0
$X(4140)$, 0^{++}	4143	0.63 ± 0.01	1.6	2.3	2.02	2.8
$X(4140)$, 2^{++}	4143	0.50 ± 0.01	6.4	8.9	8.02	11.0

TABLE IV. Cross sections and event rates for glueball candidates at LHC energies considering the theoretical decay rates presented in Ref. [12].

State	$\Gamma_{\gamma\gamma}^{\text{theor}}$(eV)	$\sigma_{Electric}$ (pb)		σ_{DZ} (pb)	
X	$X \to \gamma\gamma$	7 TeV	14 TeV	7 TeV	14 TeV
$f_0(1500)$	0.77	0.080	0.088	0.066	0.10
$f_0(1710)$	7.03	0.38	0.51	0.46	0.61
$X(1835)$	0.021	0.0009	0.0012	0.0011	0.0014

the lighter state, $f_0(1370)$, we predict large values for the total cross sections and event rates larger than 10^7 events/year at $\sqrt{s} = 7$ TeV. For the heavy X states we predict event rates larger than 10^5 events/year with a strong dependence on the quantum numbers of the state. The large values predicted by this model imply that the experimental analysis of these final states can be useful to constrain the underlying physics.

Finally, in Table IV we present our predictions for mesons which are glueball candidates, i.e., particles dominantly made of gluons. It is important to emphasize that none of them was up to now unambiguously identified. However, the existence of glueballs is predicted in many theoretical calculations, including lattice QCD (for a recent review see, e.g., Ref. [16]). In our calculations we use the two-photon decay rates proposed in Ref. [12], where the glueball production was estimated in ultraperipheral heavy ion collisions. Due to the small values of $\Gamma_{\gamma\gamma}$ for glueball states, we predict a low value for the total cross section and event rates smaller than 10^4 events/year.

Some comments are in order before the summary of our main results. Firstly, meson production in two-photon interactions are clean events, with a final state characterized by two very forward protons, the meson (or its decay products) in the central detector, and the presence of two rapidity gaps. Two rapidity gaps in the final state also are generated in central exclusive processes (CEP) by Pomeron-Pomeron interactions, where a Pomeron ($I\!P$) is associated to a colorless object (see, e.g., Ref. [17]). The magnitude of meson production in $I\!P\,I\!P$ interactions has been estimated in Refs. [18–21]. In particular, in Ref. [20], the central exclusive heavy quarkonia (χ and η) production at the LHC has been studied in detail. In comparison with our predictions for $\chi_{b,c}$ production, the results presented in [20] are at least three orders of magnitude larger. It is important to emphasize that the CEP predictions describe the CDF data for the exclusive χ_{c0} production [22]. In the case of $\eta_{b,c}$ production, the CEP predictions are a factor two larger. Consequently, we expect that for these final states the production to be dominated by $I\!P\,I\!P$ interactions. On the other hand, the production of light mesons in $I\!P\,I\!P$ interactions still is an open question, since in this case the main contribution for the cross section comes from nonperturbative regime, which implies the use of phenomenological models in order to estimate the total cross section (for some related studies see, e.g., Refs. [18,19,21]). Moreover, $I\!P\,I\!P$ cross sections are strongly dependent on the treatment of the soft final states interactions and the associated survival probability. In contrast, the predictions for light meson production in $\gamma\gamma$ interactions are much less sensitive to these effects. They are under theoretical control and can be considered a lower bound for the

event rates of these final states. Another aspect which we would like to comment is the experimental separation among $I\!P\,I\!P$ and $\gamma\gamma$ interactions. For both cases the t-distribution is of the type $\exp(-bt)$. The main distinction is associated to the slope b which is almost 4 (40) GeV^{-2} for $I\!P\,I\!P$ ($\gamma\gamma$) interactions [17,23,24]. It implies that photon-induced interactions take place larger impact parameters (i.e., are less central) than Pomeron induced processes and, consequently, the exchanged squared momentum is smaller. As a consequence it is expected that the transverse momentum distribution of the scattered protons to be different $\gamma\gamma$ and $I\!P\,I\!P$ interactions, with the latter predicting large p_T values. This expectation is corroborated by the results presented, for instance, in Refs. [23,25], where the transverse momentum distribution has been quantified considering different final states. Certainly, this subject deserves more detailed studies. However, it is important to emphasize that the ATLAS and CMS collaborations have a program of forward physics with extra detectors located in a region away from the interaction point, which probably can eliminate many serious backgrounds.

In summary, in this Brief Report we estimated the the meson production in two-photon interactions at CERN-LHC, which is characterized by two rapidity gaps in the final state. We have obtained non-negligible values for the total cross sections, which implies that the experimental study is feasible. In particular, our results indicate that this process can be useful to test the glueball and hadronic molecule models.

This work was supported by CNPq, CAPES, and FAPERGS, Brazil.

[1] S. J. Brodsky, T. Kinoshita, and H. Terazawa, Phys. Rev. D **4**, 1532 (1971); H. Terazawa, Rev. Mod. Phys. **45**, 615 (1973).
[2] N. N. Achasov and G. N. Shestakov, Phys. Usp. **54**, 799 (2011).
[3] G. Baur, K. Hencken, and D. Trautmann, J. Phys. G **24**, 1657 (1998).
[4] C. A. Bertulani, Phys. Rev. C **79**, 047901 (2009).
[5] G. Baur, K. Hencken, D. Trautmann, S. Sadovsky, and Y. Kharlov, Phys. Rep. **364**, 359 (2002); V. P. Goncalves and M. V. T. Machado, Mod. Phys. Lett. A **19**, 2525 (2004); C. A. Bertulani, S. R. Klein, and J. Nystrand, Annu. Rev. Nucl. Part. Sci. **55**, 271 (2005); K. Hencken *et al.*, Phys. Rep. **458**, 1 (2008).
[6] V. M. Budnev, I. F. Ginzburg, G. V. Meledin, and V. G. Serbo, Phys. Rep. **15**, 181 (1975).
[7] J. Nystrand, Nucl. Phys. A **752**, 470 (2005).
[8] M. Drees and D. Zeppenfeld, Phys. Rev. D **39**, 2536 (1989).
[9] B. A. Kniehl, Phys. Lett. B **254**, 267 (1991).
[10] K. Nakamura *et al.* (Particle Data Group), J. Phys. G **37**, 075021 (2010).
[11] M. Nielsen, F. S. Navarra, and S. H. Lee, Phys. Rep. **497**, 41 (2010).
[12] M. V. T. Machado and M. L. L. da Silva, Phys. Rev. C **83**, 014907 (2011).
[13] T. Branz, T. Gutsche, and V. E. Lyubovitskij, Phys. Rev. D **80**, 054019 (2009).
[14] T. Branz, L. S. Geng, and E. Oset, Phys. Rev. D **81**, 054037 (2010).
[15] T. Branz, T. Gutsche, and V. E. Lyubovitskij, Phys. Rev. D **82**, 054010 (2010).
[16] V. Crede and C. A. Meyer, Prog. Part. Nucl. Phys. **63**, 74 (2009).
[17] M. G. Albrow, T. D. Coughlin, and J. R. Forshaw, Prog. Part. Nucl. Phys. **65**, 149 (2010).
[18] A. Szczurek and P. Lebiedowicz, Nucl. Phys. A **826**, 101 (2009).
[19] M. V. T. Machado, Phys. Rev. D **86**, 014029 (2012).
[20] L. A. Harland-Lang, V. A. Khoze, M. G. Ryskin, and W. J. Stirling, Eur. Phys. J. C **69**, 179 (2010).
[21] L. A. Harland-Lang, V. A. Khoze, M. G. Ryskin, and W. J. Stirling, Eur. Phys. J. C **72**, 2110 (2012).
[22] T. Aaltonen *et al.* (CDF Collaboration), Phys. Rev. Lett. **102**, 242001 (2009).
[23] K. Piotrzkowski, Phys. Rev. D **63**, 071502 (2001).
[24] D. d'Enterria and J.-P. Lansberg, Phys. Rev. D **81**, 014004 (2010).
[25] O. Kepka and C. Royon, Phys. Rev. D **78**, 073005 (2008).